Fabrication and Replication of Polymer Integrated Optical Devices Using Electron-Beam Lithography and Soft Lithography†

Yanyi Huang,* George T. Paloczi, and Amnon Yariv

Department of Applied Physics, California Institute of Technology, Pasadena, California 91125

Cheng Zhang

Pacific Wave Industries Ltd., 129 Sheldon Street, El Segundo, California 90245

Larry R. Dalton

Department of Chemistry, University of Washington, Seattle, Washington 98195

Received: January 19, 2004

Polymeric integrated optical devices, including microring resonator optical filters and Mach−Zehnder interferometer modulators, fabricated by electron-beam lithography and soft lithography are considered in this article. Microring resonator optical filters made of SU-8 (MicroChem, Newton, MA), directly patterned by electron-beam lithography, demonstrate that SU-8 is a good candidate for high-precision, easily fabricated, and good-optical-quality passive integrated optical devices. Due to the electron-beam lithography process, the coupling between the straight waveguide and the microring resonator is precisely controlled, and the critical coupling condition can be achieved. Additionally, films containing several devices patterned by electron-beam lithography are peeled from the silicon substrate, yielding ultrathin all-polymer flexible free-standing microring resonator optical filters exhibiting up to −27 dB filtering extinction. Using a PDMS stamp, molded from these electron-beam-patterned microring resonator optical filters, identical replicas are fabricated by the soft lithography molding technique. Soft lithography is also applied to active polymer materials. A short 2-mm active-section prototype Mach−Zehnder interferometer modulator is made by the replica molding process, using CLD-1/APC electrooptic polymer as the core material. A reasonable intensity-modulation effect is observed by applying voltage to one arm of the interferometer.

1. Introduction

In the fields of high-speed telecommunication, optical signal processing, optical computing, and networking, planar integrated optical devices are the key functional devices to carry and manipulate signals. At present, semiconductor, glass-based materials and some inorganic crystals serve as both passive and active materials for making modern integrated optical devices. Polymers have become one of the most promising candidates for new materials with excellent optical performance and functionality.[1−3] Compared with other materials, polymeric materials have several advantages. First, the properties of polymers can be widely tuned by chemically modifying the structure of the monomer, the functional groups or chromophores, or the polymer backbones. Second, polymeric materials can be easily manipulated by several conventional or unconventional fabrication techniques such as dry etching,[4] wet etching,[5] embossing,[6] and soft lithography.[7] Third, compared to fragile glass fiber and expensive semiconductor chips, polymeric materials provide for easy, low-cost, and reliable fabrication of optical devices. Fourth, functional polymeric materials also provide an excellent platform for integrating several diversified materials with different functions. Low-optical-loss polymer materials for waveguiding have been studied for more than two decades, and some have been commercialized. Furthermore, several classes of active materials, such as laser-emissive and electrooptical materials,[8] can be either made as polymer or doped within the polymer matrix to become a guest−host polymer system.

Electron-beam lithography has been applied as one of the most effective methods for modern micro- and nano-fabrication. Electron-beam lithography utilizes the effect that some materials will undergo chemical changes when exposed to a beam of energetic electrons. This method has been used to fabricate high-precision optical waveguide devices, which are impossible to make by photolithographic techniques.[9] These structures typically have cross-section dimensions on the order of micrometers and minimum features on the nanometer scale. An advantage of this technique is that the waveguiding core structures are directly patterned by the electron-beam. Alternatively, soft lithography, which utilizes a master device to generate several soft molds each used to reproduce identical replicas, has been extensively developed during the past 10 years and has shown promise for improving optical waveguide manufacturing throughput.[10] This simple method has been applied in a number of fields to transfer and reproduce micro- or nanometer patterns and features. The limiting feature size can be on the order of 1 nm,[11] indicating that soft lithography is a competitive technique for producing high-quality polymer integrated optical devices.

We demonstrate two types of important integrated optical components in this report: microring resonators and Mach−

† Part of the special issue "Alvin L. Kwiram Festschrift".

* To whom correspondence should be addressed. E-mail: yanyi@caltech.edu.

10.1021/jp049724d CCC: $27.50 © 2004 American Chemical Society
Published on Web 05/01/2004

SCHEME 1: The Structure of a Microring Resonator Optical Filter

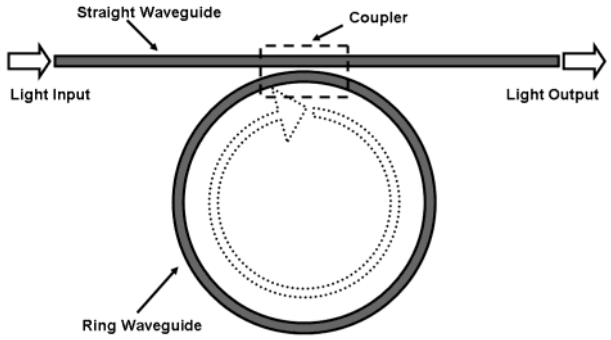

SCHEME 2: The Structure of a Mach−Zehnder Interferometer Modulator

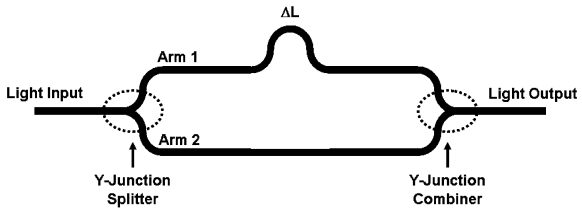

Zehnder interferometer modulators. The fabrication techniques we use here are electron-beam lithography and soft lithography. The former method is used to make either the actual device for applications or the master device for mold-making, while soft lithography is used for making a replica using either the same material as the master or transferring the structure to different materials. Microring resonators can be used as high-performance optical filters to selectively block or pass certain wavelengths.[12,13] The simplest model of the structure of a microring resonator filter is shown in Scheme 1. A straight waveguide bus channel is evanescently coupled to a filtering waveguide ring. Scheme 2 shows the structure of the Mach−Zehnder interferometer. The incoming optical signal is equally split into two waveguides by a "Y-junction" splitter and recombined with another "Y-junction" combiner. Light in one of the two arms is delayed by a certain time T because of a difference in the effective optical path lengths ΔL. ΔL can be controlled by applying a voltage across either or both of the electrooptic waveguides, changing the refractive index of the waveguide. The output signal, which results from the interference of the signals from the two separate arms, is completely controlled by the applied voltage. Controlling this applied voltage, the normalized output intensity can be swept from 0 to 1, making this device useful as an optical intensity modulator.

We also present a soft molding technique for replication of the ring resonator devices from a master device made by electron-beam lithography. Measurements show good agreement between the master device and the replicas. This result demonstrates the high fidelity of this method for making integrated optical devices and suggests that it can be a promising technique for reducing the fabrication cost by replicating many devices from a single master. To achieve active optical signal switching, we apply the soft lithography method to a guest−host second-order nonlinear optical polymer to make a prototype miniature Mach−Zehnder interferometer modulator. This demonstration shows that the soft-molding technique not only exhibits ultrahigh resolution and high replication fidelity, but also can be universally applied to many kinds of polymeric materials, both passive and active. This advantage provides the future possibility of fabricating complex or hybrid multifunctional polymeric integrated optical devices/circuits by multistep molding of different materials. Furthermore, all-polymer films containing many devices can be peeled from the solid substrate to form a flexible free-standing ultrathin sheet. These free-standing devices can be transferred to other foreign substrates without damage.

2. Experimental Section

2.1. Materials. High-contrast negative tone photoresist NANO SU-8 2000 (**1**) is purchased from MicroChem (Newton, MA). UV-curable epoxy UV15, which serves as the lower cladding of the integrated optical devices, is purchased from Master Bond Inc. (Hackensack, NJ). Epo-Tek OG-125, a low-refractive-index UV-curable epoxy, is provided by Epoxy Technology (Billerica, MA) and is used as upper cladding for our devices. The host polymer Poly[Bisphenol A carbonate-*co*-4,4′-(3,3,5-trimethylcyclohexylidene)diphenol carbonate] (APC) (**2**) is purchased from Aldrich. The electrooptic guest molecule, CLD-1 (**3**), is synthesized through the method published previously.[14] CLD-1 and APC (1:4 ratio in weight) are well dissolved in trichloroethylene to form an 11 wt % solution and filtered by 0.2 μm filter before use. Poly(dimethylsiloxane) (PDMS) is purchased from GE Electronics (RTV615 Kit) and contains a 10:1 ratio (w/w) of a mixture of prepolymer and catalyst regent. The substrate, Si and SiO_2-coated Si wafers, are purchased from Wafer World Inc. (West Palm Beach, FL).

SCHEME 3: The Chemical Structures of Materials

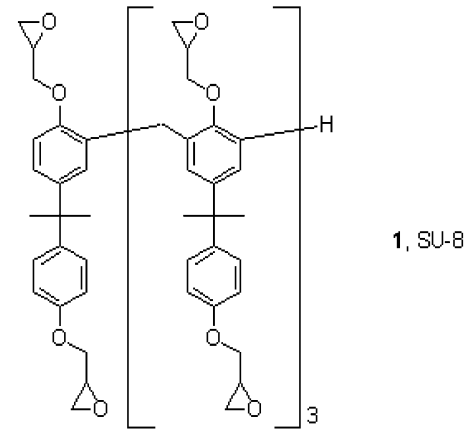

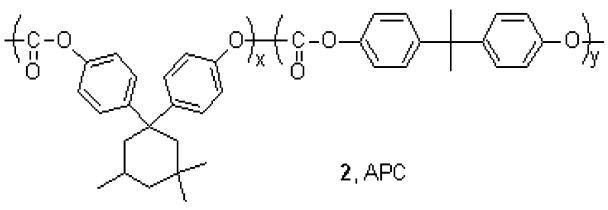

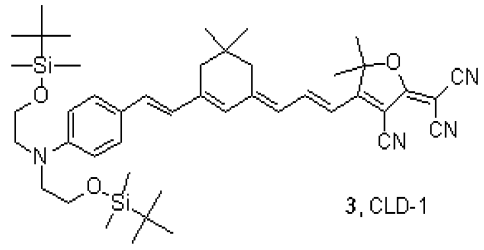

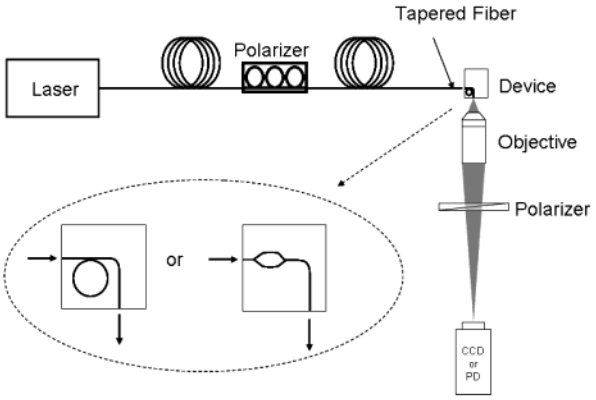

Figure 1. The measurement setup for polymeric integrated optical devices.

2.2. Fabrication and Measurements. A Hitachi S-4100 field-emission scanning electron microscope with NPGS (Nanometer Pattern Generation System, J. C. Nabity Lithography Systems, Bozeman, MT) is employed for electron-beam lithography. The SU-8 resist is patterned by direct electron-beam writing and developed by SU-8 developer (propylene glycol monomethyl ether acetate (PGMEA), MicroChem, Newton, MA). The SU-8 pattern can serve as the measured device, or soft molds can be made from the SU-8 master pattern to fabricate the replicas. The replicas are made by stamping the soft mold on top of the polymer solution/precursor and then curing it. The molding pressure is measured by a force gauge to ensure the same fabrication conditions for each stamping. The patterned device can be clad by spin-coating a polymer of lower refractive index as required for single-mode transmission. The substrates are cleaved on a cleaving station (Karl Suss HR-100), forming good optical quality waveguide end-facets for coupling light from free-space or through tapered fibers. The samples which use UV15 as the lower cladding layer can be peeled from the gold substrate to form ultrathin free-standing flexible polymer optical devices. Such free-standing devices are easily transferred to other substrates with minimal change in the optical functions. The optical microscope images are taken through an Olympus BX51 microscope, while the scanning electron microscope (SEM) images are taken with a Hitachi S4100 SEM.

The measurement setup for the polymer optical integrated devices is shown in Figure 1. Light from a wavelength-tunable laser (8164B, Agilent) is passed through a polarizer before being launched into the devices via a tapered single-mode fiber. The device output is collected by a 20× aspherical microscope objective (New Focus, San Jose, CA) focused on either an infrared CCD camera (C2730, Hamamatsu, Japan) or an infrared photoreceiver (New Focus, San Jose, CA). The coupling between the tapered fiber and the input facet of the waveguide is optimized for each measurement. The voltage applied to the modulator devices are generated by a sourcemeter (2400, Keithley, Cleveland, OH). The signal from the photoreceiveris collected by a digital multimeter (2000, Keithley, Cleveland, OH). The signal is normalized for each measurement. The entire setup is controlled by MATLAB via general purpose instrumentation bus (GPIB).

3. Results and Discussion

3.1. Microring Optical Resonators. By using electron-beam lithography, integrated optical devices can be directly patterned in SU-8 epoxy. SU-8 has a relatively high refractive index (1.565 at 1550 nm) and low loss (less than 1 dB/cm) when it is cured. It also has excellent mechanical properties responsible for good optical quality waveguide end-facets when the substrate is cleaved. Hence SU-8 has become a useful material for polymer integrated optical devices. To provide high-refractive-index contrast, we choose for the substrate a silicon wafer with 5 μm thermally grown amorphous silica ($n = 1.445$ at 1550 nm). SU-8 pre-polymer solution is spun on top of the substrate to form a 2-μm thick layer. By electron-beam exposure and developing with PGMEA, we fabricate the microring resonator devices as is shown in Figure 2. No upper cladding is applied to the directly patterned resonators. The cross-section of the waveguide is approximately 2 × 2 μm. The finite-difference mode solving calculations show that our structure is appropriate for single-mode operation around 1550 nm.

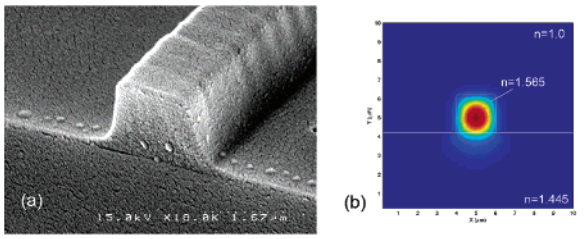

Figure 2. (a) SEM image of the end-facet of the SU-8 waveguide on a silica-coated silicon substrate. (b) The finite-difference mode-solver simulation of the structure we made. The contour shows the amplitude of light electrical field, indicating the single-mode guiding condition in our structure.

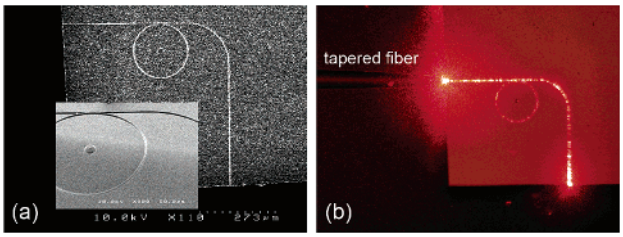

Figure 3. SEM image (a) and optical microscopic image (b) of the SU-8 microring resonator optical filter on silica cladding layer. In (a), the inset shows the details of coupling region of device. In (b), a He−Ne laser is injected into the waveguide for demonstration.

The structure of the microring resonator optical filter device is fabricated to have perpendicular input and output waveguides for easier measurement of the output signal without the influence of scattering from input. Figure 3 shows microscope images of this device. The diameter of the microring is 200 μm and the gap between the ring resonator and the straight waveguide is 250 nm. Figure 4 shows the measured spectral transmission of this device. The result shows that this microring resonator device has repeated notches with a separation (free spectral range, FSR) of 2.45 nm. The notch extinctions are about −9 dB for a relatively wide spectral region in the telecommunications band. These spectral features are typical of a waveguide evanescently coupled to a microring resonator. When two waveguides are placed in close proximity to one another, the light propagating in one waveguide will partially couple into the other waveguide. The final ratio of light coupled from one waveguide to the other is determined by the refractive indices of the materials in the coupling region and the separation between the two waveguides. In the devices we made, light is injected into the straight waveguide, and partially coupled into the ring resonator by this coupling mechanism. Based on a beam propagation method (FFT-BPM) algorithm, we simulate the coupling region between the straight bus waveguide and the curved section of the ring

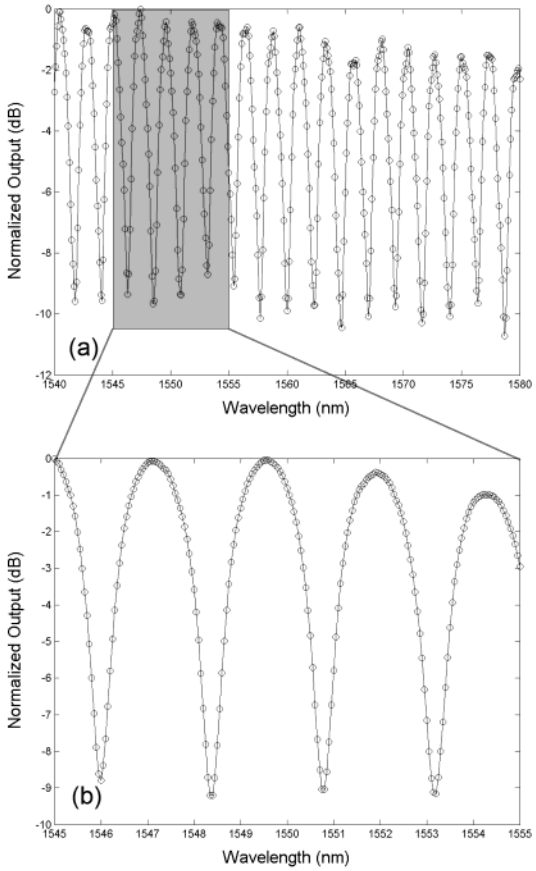

Figure 4. Transmission spectra of 200-μm diameter microring resonator filter. (a) Spectrum with large scanning region, (b) the spectrum with higher resolution but narrower scanning region.

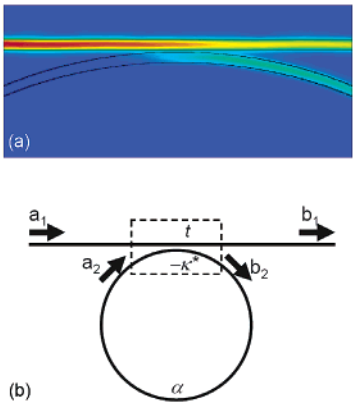

Figure 5. (a) Beam propagation method simulation of the coupling region of the microring resonator optical filter. (b) The schematic geometry for analysis of the microring resonator optical filter.

resonator. Figure 5a shows the FFT-BPM simulation result of the coupling region of the microring resonator optical filter. By reciprocity, a portion of the light propagating in the ring couples back to the straight waveguide. The coupling matrix[12] that describes the coupling region (see Figure 5b) is

$$\begin{bmatrix} b_1 \\ b_2 \end{bmatrix} = \begin{bmatrix} t & \kappa \\ -\kappa^* & t^* \end{bmatrix} \begin{bmatrix} a_1 \\ a_2 \end{bmatrix} \tag{1}$$

where t gives the field amplitude not coupled and κ, the coupling coefficient, determines the field amplitude coupled into or out of the resonator. Energy conservation requires

$$|t|^2 + |\kappa|^2 = 1 \tag{2}$$

The light propagating in the microring is subject to the round trip condition

$$a_2 = \alpha e^{i\theta} b_2 \tag{3}$$

where α defines the field amplitude remaining after one circulation of light propagation, and θ is phase shift after one circulation. Combining these three equations, the transmission function of the device can be written as

$$|\frac{b_1}{a_1}|^2 = \frac{\alpha^2 + |t|^2 - 2\alpha|t|\cos\theta}{1 + \alpha^2|t|^2 - 2\alpha|t|\cos\theta} \tag{4}$$

For certain wavelengths, the phase accumulated in a circulation θ is equal to $2m\pi$ (m is an integer). In this case, the field returning to the coupler from the ring, after traversing the ring length, interferes destructively with the field impinging on the coupler from the straight waveguide. If the amplitudes of the interfering fields are equal, the destructive interference is complete, and the output of the straight waveguide vanishes. Simultaneously, the field in the resonating ring is built up because of the constructive interference between the light field before and after circulation. Mathematically, in the static state, at resonance $\theta = 2m\pi$, we can rewrite eq 4 as

$$|\frac{b_1}{a_1}|^2 = \frac{(\alpha - |t|)^2}{(1 - \alpha|t|)^2} \tag{5}$$

Clearly, under the resonant condition, the quality of the filter depends on α and $|t|$. If one wants to have an entirely vanishing output, the relationship $\alpha = |t|$ is required. This equality is called the *critical coupling* condition. In a particular device, once the ring resonator has been made, α is determined. Thus, to achieve critical coupling requires tuning of the coupling between the straight waveguide and the ring. Given the passive waveguiding material, the coupling between the straight waveguide and the microring resonator is adjusted by changing the gap between them. According to our measurement (Figure 4), a 250-nm gap between the straight waveguide and the microring causes a ca. −10 dB signal extinction of the filter device, indicating that the critical coupling condition is essentially achieved.

3.2. Soft Lithographic Replication of Microring Resonator Optical Filter. Since the critical coupling condition is very sensitive to the gap between the straight waveguide and the microring resonator, a high-precision fabrication technique is required for reproducing identical structures. Although electron-beam lithography is among the best choices for making such devices, it requires a multistep process with relatively complex equipment and makes fabrication high-cost. We apply the soft lithography technique as our new choice to reproduce high-quality microring resonator filter devices because this fast, low-cost fabrication technique provides nanometer precision, which is required for integrated optical device manufacturing. The waveguide core material used for the replica microring resonator optical filters is the same as the master devices to allow for easy comparison. The replica device is easily cured by ultraviolet (UV) light due to the rapid curing of SU-8 under UV illumination and the transparency of PDMS to UV light. The flowchart of the soft lithography reproduction process is shown as Figure 6.

The transmission spectrum of the soft lithographic replica is compared with the master device, as shown in Figure 7. The shapes of the two transmission spectra, including the slope of

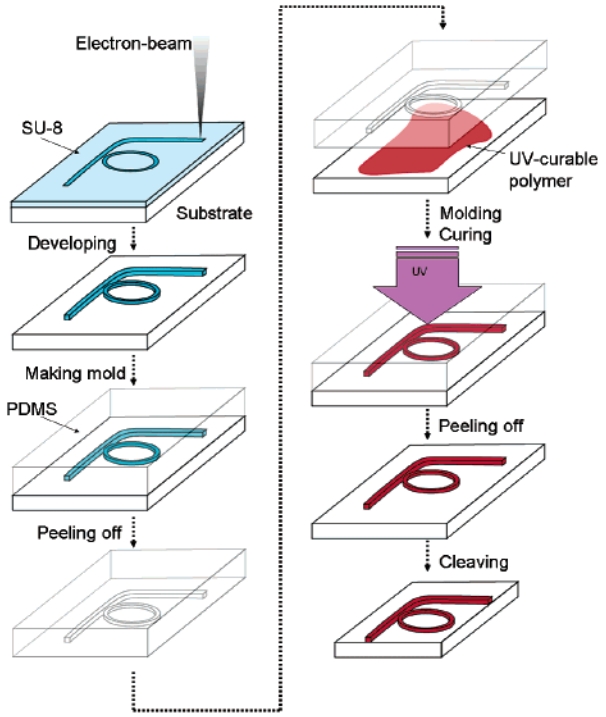

Figure 6. Schematic flowchart showing electron-beam lithographic fabrication of a microring resonator filter and its soft lithographic replication.

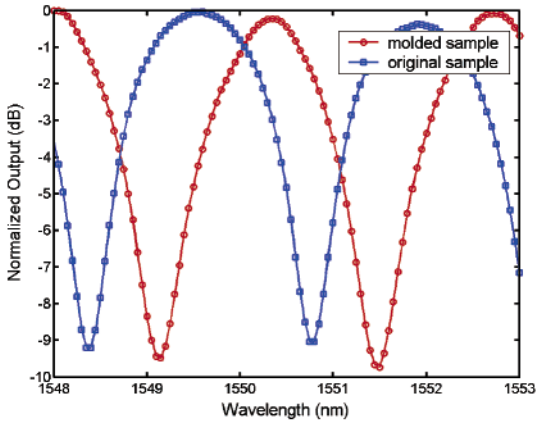

Figure 7. Comparison between the transmission spectra of the master microring resonator optical filter and its soft lithographic replica.

the notches and the extinction ratios, are very similar, indicating the molded device is a close copy of the master device. As discussed above, the extinction of the transmission notches is extremely sensitive to the precision of the fabrication technique. Both spectra of the master device and the replicated device exhibit −9 to −10 dB extinction ratios, confirming the high reliability of the soft lithography process.

A noticeable difference between the two transmission spectra is the lack of alignment in the notch positions of the replica and the master devices. This dissimilarity is attributed to the slightly different free spectral ranges of the two rings due to slightly different waveguide effective refractive indices. According to the different notch wavelengths in Figure 7, the difference between the effective refractive indices is 0.0007. In practical applications, this difference can be trimmed by using active materials instead of the passive SU-8 we present here. There are several possible reasons for this change of the effective refractive index during the reproduction process, such as minor distortion of PDMS mold and unevenness of the materials. The most probable reason might be that the soft molding technique always leaves some residual background material on the substrate.[15] Although this background can cause this change of the effective refractive index, in most cases it will not adversely affect the optical propagation in polymeric waveguides.[16]

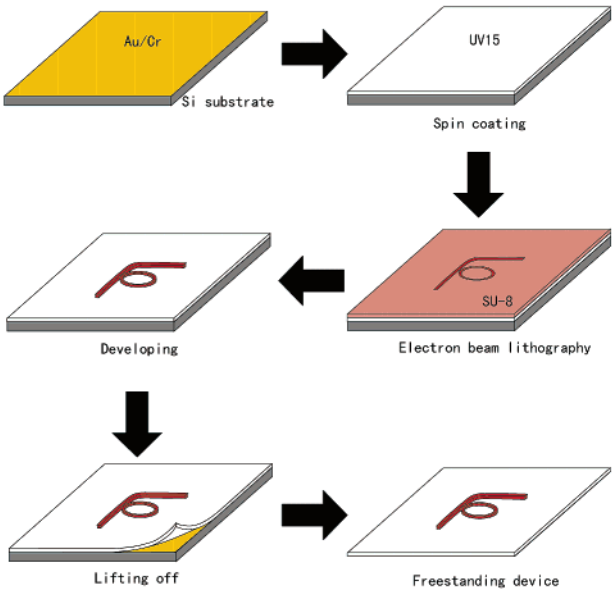

Figure 8. Schematic diagram of the fabrication process of free-standing all-polymer integrated optical devices.

3.3. Flexible Free-Standing All-Polymer Ultrathin Microring Resonator Optical Filter. As pointed out above, polymer materials can be chemically synthesized to fit various requirements for different applications. Specifically, different chemical structures of polymer will provide different optical properties. At present, the refractive index of optical polymer material can be varied from 1.3 to 1.7, indicating we can easily employ different polymer materials as both cladding material and core material to match the required refractive index contrast.[1−3] Actually, it is most common that polymers are used for both the core and cladding layers, rather than mixed crystal-, or glass−polymer material systems. Despite all of the optically relevant materials being polymer, most of the devices remain on solid substrates. One of the special intrinsic properties of polymer materials is that they are much softer than glass or crystalline materials. This property makes it possible to fabricate mechanically flexible and transparent integrated optical devices and circuits. Recently, Steier et al. reported a method to lift-off a flexible polymer modulator from a solid substrate.[17] We will demonstrate here a simpler method to fabricate a much thinner (∼10 μm) all-polymer device, which is flexible and transferable easily to foreign substrates without distorting the optical functions of the devices.

The fabrication method is briefly described in Figure 8. The critical point here is to utilize the weak adhesion between Au and the UV15 polymer film, which serves as the lower cladding due to its lower refractive index (1.504 at 1550 nm). A thin (5−10 nm) Cr layer is evaporated between the Au and the silicon substrate to improve the adhesion. After developing the devices, the whole polymer structure, several square centimeters in extent, can be peeled off. Figure 9 shows several examples of flexible polymer integrated optical devices made by this method. Individual flexible devices can be transferred to other substrates by heating. Figure 9c demonstrates a microring resonator device adhered to the outer surface of a 0.8 mm diameter capillary tube. The possibility of adhering polymeric integrated optical devices to arbitrary surfaces is not only useful

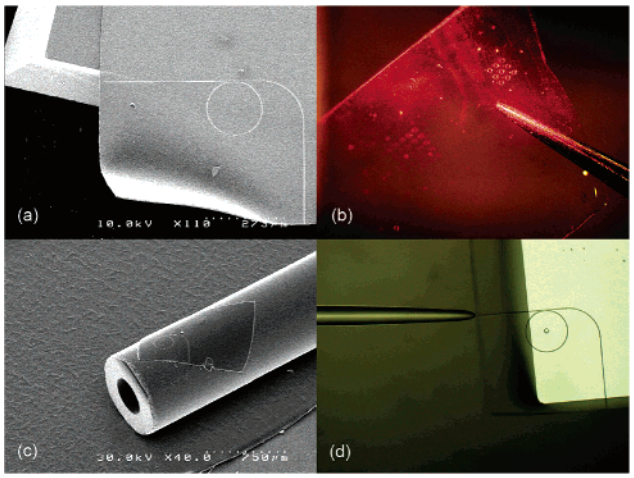

Figure 9. Free-standing polymeric integrated optical devices. (a) SEM image of the free-standing polymeric microring resonator optical filter. (b) The free-standing sheet of a polymeric mirroring array. (c) A microring resonator optical filter transferred onto a capillary tube. (d) The optical microscopic image on the free-standing polymeric microring resonator optical filter during measurement. The white section in the picture is the silicon wafer under the polymeric device for support.

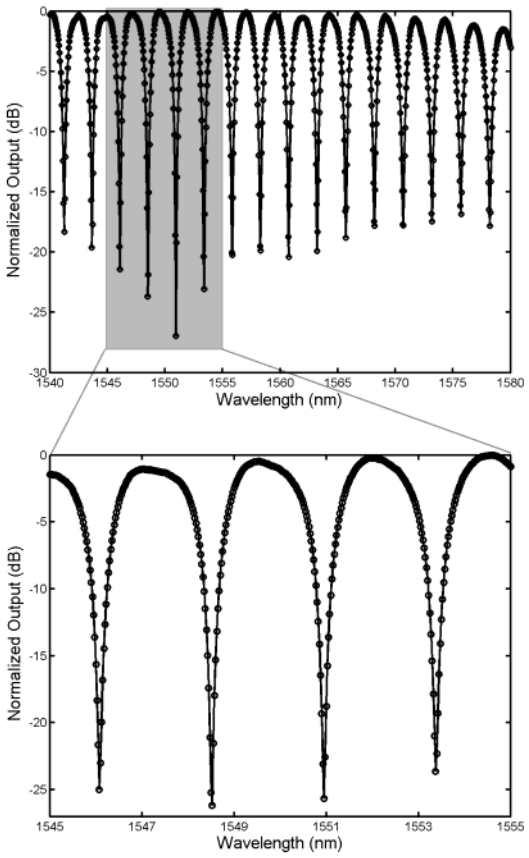

Figure 10. The transmission spectra of the free-standing polymeric microring resonator optical filter.

for making nonflat optical circuits, but also promising for fabricating hybrid functional devices or circuit containing both polymeric materials and other active materials.

For measuring the flexible polymeric microring resonator optical filter, we use a piece of silicon wafer to partially support the device, as seen in Figure 9d. The transmission spectra are shown as Figure 10. The notch extinction (up to −27 dB) indicates that the critical coupling condition is very nearly achieved in this device. Numerical fitting of experimental data

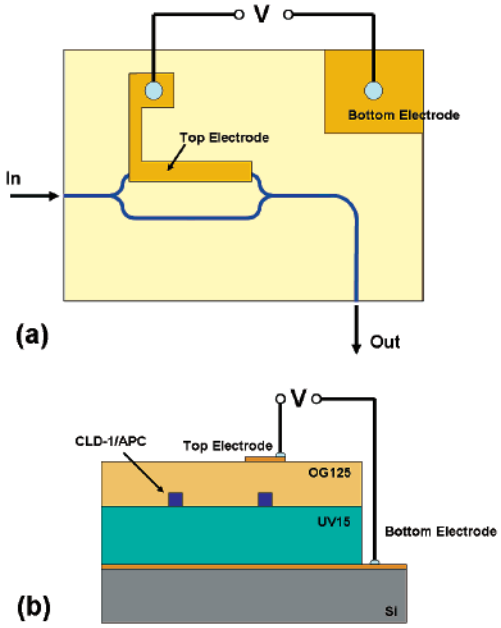

Figure 11. The structure of the polymeric Mach−Zehnder interferometer modulator. (a) Top view. (b) Side view.

gives the parameters of our device: $\alpha = 0.56$, $t = 0.54$, FSR = 2.435 nm, and effective refractive index 1.508. The loaded quality factor (Q) of this device can be calculated from the experimental data as around 2×10^3. The notch extinction, which represents the quality of filtering, is beyond the requirement of practical telecommunications applications. The Q factor can be improved by choosing other compatible materials for better optical field confinement in the waveguide and therefore decreasing the bend loss.

3.4. Soft Lithographic Polymeric Mach−Zehnder Interferometer. By using a procedure similar to that described in sections 3.1 and 3.2, we can fabricate active polymeric integrated optical devices by soft molding second-order nonlinear optical polymer materials. Here we demonstrate a prototype Mach−Zehnder interferometer modulator fabricated by soft lithography. The structure of the device and dimensions are shown in Figure 11. A guest−host material, CLD−1/APC, is used as the electrooptically active polymeric material core. The total length of the active section of the interferometer, limited by the electron-beam lithography system, is restricted to 2 mm. We directly pattern the master Mach−Zehnder interferometer in a 2-μm SU-8 film on a silicon substrate. After developing and hard baking, this structure is used to make the PDMS mold.

A 200-nm thick Au layer was deposited onto the Cr-coated (10 nm) silicon substrate, serving as the bottom electrode. UV15 (5 μm) is spun onto the Au, serving as the lower cladding. After 1-min UV exposure and post baking at 310 K for 30 min, the UV15 cladding is fully cured. A drop of CLD-1/APC guest−host polymer, dissolved in trichloroethylene solution, is placed onto the UV15 cladding layer and stamped by the PDMS mold with pressure 2×10^5 Pa for 20 min to form the core waveguide. After the PDMS mold has been released, OG-125 (3 μm) is spun on the molded device serving as the upper cladding.

After the OG-125 layer is cured by UV exposure, the entire structure is heated to the glassy temperature of APC (ca. 410 K) and poled by a corona poling setup. The poling voltage is set to 8 kV, and the distance between the corona electrode and the sample is 2 cm. The temperature is increased to 420 K, and both the temperature and poling voltage are kept constant for 30 min. The poling voltage is applied continuously while the

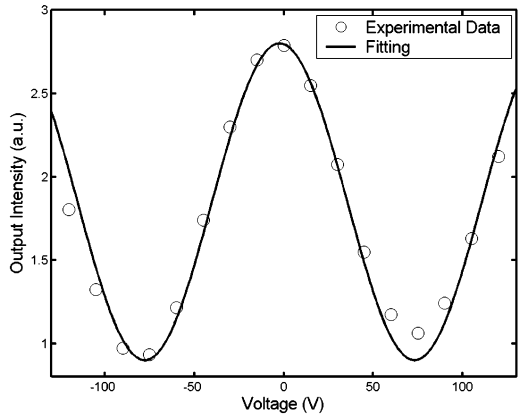

Figure 12. Halfwave voltage measurement from a 2-mm soft lithographic Mach−Zehnder interferometer modulator device.

temperature is allowed to drop to room temperature, fixing the orientation of the chromophores in the polymer waveguide. The concentration of the second-order nonlinear optical chromophore CLD-1 is optimized for the best electrooptic effect according to the investigation on the competition of intermolecular electrostatic and poling-field interactions for guest−host polymer materials.[18]

The measurement setup of the Mach−Zehnder interferometer modulator device is similar to that of the microring resonator, except the wavelength is fixed and a voltage is applied to one arm of the modulator. The intensity of the output signal is changed by the applied voltage, as shown in Figure 12. The figure shows that the halfwave voltage (V_π) of our modulator is about 80 V. This number is unacceptably high for practical applications;[19] however, there are several reasons for this high value. The practical figure of merit for electrooptic modulators is the halfwave voltage times the active length, $V_\pi \cdot L$. In our case this figure of merit is 0.16 V m, corresponding to a V_π of 8 V for a 2 cm active section. The voltage will also be proportionally reduced by reducing the overall film thickness. Optimized poling will further reduce V_π. Finally, using a push−pull electrode configuration will result in another factor of 2 reduction in V_π. Accounting for these considerations, our results indicate that soft lithography is suitable for making low-cost, high fabrication throughput polymeric optical intensity modulators. Further experiments are in progress to improve the performance of polymeric modulator devices as described.

4. Conclusions

Microring resonator optical filters and Mach−Zehnder interferometer modulators made in polymeric materials have been demonstrated as model devices for passive and active polymeric integrated optical devices using novel fabrication techniques. By direct electron-beam patterning of SU-8 photoresist, passive polymeric integrated optical devices are made on a proper substrate. Using replica molding, these structures can be transferred onto other substrates with either the same or different materials. The comparison between the master microring resonator optical filter and its PDMS-molded replica demonstrates the high resolution and high fidelity of the soft lithographic replication technique. By utilizing the weak adhesion between the lower cladding UV15 epoxy and a Au-coated substrate, a SU-8 microring resonator optical filter was peeled from the solid substrate to create free-standing all-polymer integrated optical devices. These free-standing devices can be transferred onto foreign substrates while still exhibiting high-quality filtering properties. This ability provides the possibility of easily making flexible, nonflat and/or hybrid polymeric integrated optical devices. By using PDMS replica molding, active polymer materials were patterned to form high-quality and high-resolution integrated optical devices. A miniature Mach−Zehnder interferometer modulator has been made to demonstrate the possibility of soft lithography fabricated active polymeric devices. The application of combining the electron-beam lithography and soft lithography techniques improves the fabrication throughput, decreases the fabrication cost, and ensures the high-resolution requirement of polymeric integrated optical devices for practical applications.

Acknowledgment. The authors thank J. Poon, Dr. J. Scheuer, Dr. R. Lee, Prof. S. Mookherjea, W. Green, and J. Choi for kind help and fruitful discussion. The work is supported by the National Science Foundation (DMR-0120967) and the Defense Advanced Research Projects Agency (N00014-04-1-0094).

References and Notes

(1) Eldada, L.; Shacklette, L. W. *IEEE J. Select. Top. Quantum Electron.* **2000**, *6*, 54.

(2) Ma, H.; Jen, A. K.-Y.; Dalton, L. R. *Adv. Mater.* **2002**, *14*, 1339.

(3) Eldada, L.; Blomquist, R.; Shacklette, L. W.; McFarland, M. J. *Opt. Eng.* **2000**, *39*, 596.

(4) For example, see: Zhao, Y. G.; Lu, W. K.; Ma, Y.; Kim, S. S.; Ho, S. T.; Marks, T. J. *Appl. Phys. Lett.* **2000**, *77*, 2961.

(5) For example, see: Enami, Y.; Meredith, G.; Peyghambarian, N.; Jen, A. K.-Y. *Appl. Phys. Lett.* **2003**, *83*, 4692.

(6) (a) Xia, Q.; Keimel, C.; Ge, H.; Yu, Z.; Wu, W.; Chou, S. Y. *Appl. Phys. Lett.* **2003**, *83*, 4417. (b) Chao, C.; Guo, L. J. *J. Vac. Sci. Technol. B* **2002**, *20*, 2862. (c) Mizuno, H.; Sugihara, O.; Kaino, T.; Okamoto, N.; Hosino, M. *Opt. Lett.* **2003**, *28*, 2378.

(7) For example, see: (a) Xia, Y.; Whitesides, G. M. *Annu. Rev. Mater. Sci.* **1998**, *28*, 153. (b) Xia, Y.; Whitesides, G. M. *Angew Chem. Int. Ed.* **1998**, *37*, 550. (c) Xia, Y.; Rogers, J. A.; Paul, K. E.; Whitesides, G. M. *Chem. Rev.* **1999**, *99*, 1823. (d) Xia, Y.; Kim, E.; Zhao, X.-M.; Rogers, J. A.; Prentiss, M.; Whitesides, G. M. *Science* **1996**, *273*, 347.

(8) (a) Wijekoon, W. M. K. P.; Prasad, P. N. Nonlinear Optical Preperties of Polymers. In *Physical Properties of Polymers Handbook*; Mark, J. E., Ed.; AIP Press: New York, 1996. (b) Dalton, L. R.; Sterer, W. H.; Robinson, B. H.; Zhang, C.; Ren, A.; Garner, S.; Chen, A.; Londergan, T.; Irwin, L.; Carlson, B.; Fifield, L.; Phelan, G.; Kincaid, C.; Amend, J.; Jen, A. *J. Mater. Chem.* **1999**, *9*, 1905. (c) Dalton, L. *Adv. Polym. Sci.* **2003**, *158*, 1. (d) Kajzar, F.; Lee, K.-S.; Jen, A. K.-Y. *Adv. Polym. Sci.* **2003**, *161*, 1. (e) Dalton, L. R. *J. Phys. Condens. Matter* **2003**, *15*, R897.

(9) For example, see: Wong, W. H.; Zhou, J.; Pun, E. Y. B. *Appl. Phys. Lett.* **2001**, *78*, 2110.

(10) (a) Zhao, X. M.; Smith, S. P.; Waldman, S. J.; Whitesides, G. M.; Prentiss, M. *Appl. Phys. Lett.* **1997**, *71*, 1017. (b) Rogers, J. A.; Meier, M.; Dodabalapur, A. *Appl. Phys. Lett.* **1998**, *73*, 1766. (c) Rogers, J. A.; Meier, M.; Dodabalapur, A.; Laskowski, E. J.; Capppuzzo, M. A. *Appl. Phys. Lett.* **1999**, *74*, 3257.

(11) Quake, S. R.; Scherer, A. *Science* **2000**, *290*, 1536.

(12) (a) Yariv, A. *Electron. Lett.* **2000**, *36*, 321. (b) Yariv A. *IEEE Photonics Technol. Lett.* **2002**, *14*, 483. (c) Madsen, C. K.; Zhao, J. H. *Optical Filter Design and Analysis: A Signal Processing Approach;* John Wiley & Sons: New York, 1999.

(13) (a) Rabiei, P.; Steier, W. H.; Zhang, C.; Dalton, L. R. *J. Lightwave Technol.* **2002**, *20*, 1968. (b) Paloczi, G. T.; Huang, Y.; Yariv, A. *Electron. Lett.* **2003**, *39*, 1650. (c) Huang, Y.; Paloczi, G. T.; Scheuer, J.; Yariv, A. *Opt. Express* **2003**, *11*, 2452. (d) Paloczi, G. T.; Huang, Y.; Yariv, A.; Mookherjea, S. *Opt. Express* **2003**, *11*, 2666.

(14) (a) Zhang, C.; Ren, A. S.; Wang, F.; Zhu, J.; Dalton, L. R. *Chem. Mater.* **1999**, *11*, 1966. (b) Shi, Y.; Zhang, C.; Zhang, H.; Bechtel, J. H.; Dalton, L. R.; Robinson, B. H.; Sterer, W. H. *Science* **2000**, *288*, 119. (c) Shi, Y.; Lin, W.; Olson, D. J.; Bechtel, J. H.; Zhang, H.; Steier, W. H.; Zhang, C.; Dalton, L. R. *Appl. Phys. Lett.* **2000**, *77*, 1. (d) Oh, M.-C.; Zhang, H.; Zhang, C.; Erlig, H.; Chang, Y.; Tsap, B.; Chang, D.; Szep, A.; Steier, W. H.; Fetterman, H. R.; Dalton, L. R. *IEEE J. Select. Top. Quantum Electron.* **2001**, *7*, 826.

(15) Malaquin, L.; Vieu, C. Using PDMS as a Thermocurable Resist for a Mold Assisted Imprint Process. In *Alternative Lithography: Unleashing the Potentials of Nanotechnology*; Torres, C. M. S., Ed.; Kluwer Academic Publishers: Boston, 2003.
(16) Paloczi, G. T.; Huang, Y.; Yariv, A. Submitted.
(17) Song, H.-C.; Oh, M.-C.; Ahn, S.-W.; Steier, W. H.; Fetterman, H. R.; Zhang, C. *Appl. Phys. Lett.* **2003**, *82*, 4432.
(18) Robinson, B. H.; Dalton, L. R. *J. Phys. Chem. A* **2000**, *104*, 4785.
(19) (a) An, D.; Shi, Z.; Sun, L.; Taboada, J. M.; Zhou, Q.; Lu, X.; Chen, R. T.; Tang, S.; Zhang, H.; Steier, W. H.; Ren, A.; Dalton, L. R. *Appl. Phys. Lett.* **2000**, *76*, 1972. (b) Ahn, S.-W.; Steier, W. H.; Kuo, Y.-H.; Oh, M.-C.; Lee, H.-J.; Zhang, C.; Fetterman, H. R. *Opt. Lett.* **2002**, *27*, 2109. (c) Lee, M.; Katz, H. E.; Erben, C.; Gill, D. M.; Gopalan, P.; Heber, J. D.; McGee, D. J. *Science* **2002**, *298*, 1401.